Effect of Deformation Temperature on the Mechanical Behavior and Deformation Mechanisms of Al-Al_2O_3 Metal Matrix Composites

A.A. Mazen

(Submitted 21 December 1998; in revised form 1 March 1998)

Aluminum-alumina (Al-Al_2O_3) metal matrix composite (MMC) materials were fabricated using the powder metallurgy (PM) techniques of hot pressing followed by hot extrusion. Different reinforcement weight fractions were used, that is, 0, 2.5, 5, and 10 wt% Al_2O_3. The effect of deformation temperature was investigated through hot tensile deformation conducted at different temperatures. The microstructures of the tested specimens were also investigated to characterize the operative softening mechanisms.

The yield and tensile strength of the Al-Al_2O_3 were found to improve as a function of reinforcement weight fraction. With the exception of Al-10wt%Al_2O_3, the MMC showed better strength and behavior at high temperatures than the unreinforced matrix. The uniform deformation range was found to decrease for the same reinforcement weight fraction, as a function of temperature. For the same deformation temperature, it increases as a function of reinforcement weight fraction.

Both dynamic recovery and dynamic recrystallization were found to be operative in Al-Al_2O_3 MMC as a function of deformation temperature. Dynamic recovery is dominant in the lower temperature range, while dynamic recrystallization is more dominant at the higher range. The increase in reinforcement weight fraction was found to lead to early nucleation of recrystallization. No direct relationship was established as far as the number of grains nucleated due to each reinforcement particle.

Keywords	aluminum/alumina, deformation temperature, dynamic recovery, dynamic recrystallization, high temperature deformation, metal matrix composites, powder metallurgy, softening

1. Introduction

One of the major driving forces for research and development in the area of metal matrix composite (MMC) materials is the need for new high temperature resisting materials.

Materials serving at high temperatures experience several problems, for example, a greater mobility of dislocations, loss of strength, oxidation, corrosion, and so on (Ref 1). Aluminum-base MMCs are receiving considerable attention due to the many advantages they offer, for example, light weight, high strength/weight ratio, superior corrosion resistance, and superior elevated temperature mechanical behavior when compared to ingot aluminum and some conventional ingot steels (Ref 2-6).

Unidirectional fiber-reinforced MMCs proved to be expensive and have poor transverse strength (Ref 4, 6, 7). Other forms of reinforcement, for example, short fibers, whiskers, and particles are meeting wide acceptance due to their availability and low cost. Isotropic properties can also be obtained in MMCs reinforced using these forms of reinforcement.

Casting techniques are widely used to fabricate MMCs (Ref 7-9). However, cast fabricated MMCs do not exhibit substantially higher strength than that of the matrix material (Ref 10). Powder metallurgy (PM) techniques provide a powerful alternative for conventional processing. These techniques allow better control on reinforcement distribution and produce materials with superior mechanical properties (Ref 2,11).

Most of the work done and published in open literature has concentrated on Al-SiC MMCs manufactured by different techniques. Studies considering other reinforcement particles, for example alumina (Al_2O_3), iron, and so on, have been so limited to date. Moreover, almost all of the published work investigated MMCs with an aluminum alloy matrix. Few investigations were conducted with a matrix of pure aluminum. In these cases, either high percentage alumina particles were used (up to 61%), or alumina particles coated with MgO were employed as reinforcement (Ref 12-14).

The goal of the present work is to present an experimental study on the high temperature behavior of Al-Al_2O_3 MMCs manufactured using PM techniques of hot pressing followed by hot extrusion. The matrix is made of commercially pure powder, and the reinforcement is pure alumina (Al_2O_3) particles. The reinforcement weight fractions investigated range from 0 to 10 wt% Al_2O_3.

2. Experimental Procedures

2.1 Specimen Fabrication

Preweighed amounts of pure alumina (Al_2O_3) powder were mixed with preweighed amounts of commercially pure aluminum powder (Al) in a mechanical mixer. The weights of the

A.A. Mazen, Dept. of Engineering, The American University in Cairo, 113 Kasr El Aini St., PO Box 2511, Cairo 11511, Egypt.

powders were calculated to achieve specimens of the following compositions: Al-0wt%Al_2O_3, Al-2.5wt%Al_2O_3, and Al-10wt%Al_2O_3. No additives or catalysts were added to the mixtures. Each mixture was hot pressed at a temperature of 873 K, which was maintained at a maximum compaction stress of 150 MPa for 3 h. The produced billets were then hot extruded at an extrusion ratio of 5 to 1 to impart densification. The extruded bars were used as raw stock out of which specimens were machined. Figure 1 shows a photograph of a powder mixture, hot pressed billets, extruded bars, and machined test specimens.

2.2 Testing and Characterization

To determine the mechanical behavior of the different materials as a function of deformation temperature, hot tensile tests were conducted at a constant strain rate of 10^{-3} s^{-1}. The range of testing temperatures was room temperature (298 K), 200 °C (473 K), 250 °C (523 K), and 300 °C (573 K). These testing temperatures are equivalent to 0.32, 0.56, and 0.6 T_m, respectively, where T_m is the melting point of the aluminum matrix. This range includes the upper bound of recovery temperatures and goes well into the recrystallization temperatures of pure aluminum (Ref 15). Different sections of the tested specimens were cut and prepared for microstructural examinations by mounting in cold resin mount followed by careful polishing and etching.

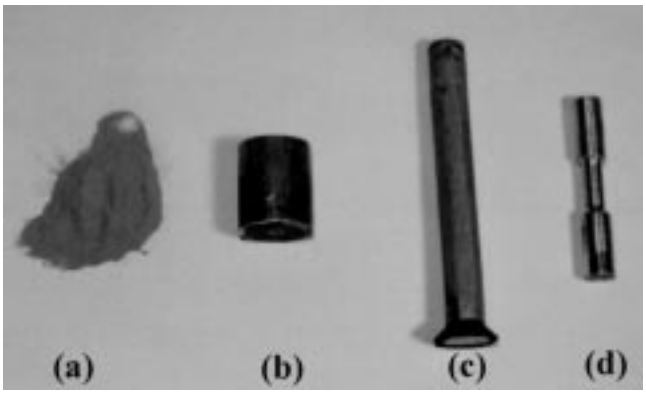

Fig. 1 (a) Powder mixture. (b) Hot pressed billets. (c) Extruded bars. (d) Machined tension test specimen

3. Analysis and Discussion of Results

3.1 Mechanical Behavior of Al-Al_2O_3 MMC

Figures 2(a) through (d) show the conventional plastic stress-strain curves for different materials at each of the testing temperatures. At room temperature (298 K) work hardening dominates the plastic deformation behavior for all compositions (Fig. 2a). In the absence of thermal activation, the mechanism of plastic deformation is slip by dislocation motion. As these dislocations pile up against barriers to their motion they entangle, causing resistance to further deformation, that is, strain hardening (Ref 15). The Al-2.5wt%Al_2O_3 shows reduction in strength compared to the unreinforced matrix (Al-0wt%Al_2O_3). This is the result of ineffective strengthening due to smaller weight fraction of reinforcement than the minimum weight fraction required to induce strengthening (Ref 16, 17). In a previous study (Ref 18), Mazen and Ahmed found that the minimum reinforcement weight fraction needed for strengthening in an Al-Al_2O_3 MMC is 3.4 wt% alumina. Improvement in strength was obtained for the Al-5wt%Al_2O_3 and Al-10wt%Al_2O_3 MMCs. Hardening due to plastic deformation at room temperature still dominates the deformation for all material compositions.

At higher temperatures, as shown in Fig. 2(b) (473 K), 2(c) (523 K), and 2(d) (573 K), the tensile plastic stress-strain curves for all compositions exhibit initial hardening up to a maximum load, followed by softening till fracture. The strain range dominated by strain hardening decreased as the deformation temperature increased, thus, it is temperature dependent. This is due to stress relaxation at matrix/particle interfaces and the enhancement of recovery processes at these interfaces (Ref 19). However, it does not seem to be highly sensitive to rein-

Table 1 Summary of mechanical deformation parameters of Al-Al_2O_3 MMC

Material	*T*, K	S_y, MPa	S_u, MPa	El., %	ε_u	Post ε_u	(ε_u/%El.), %	*n*
Al-0wt%Al_2O_3	298	61.9	133.96	17.90	17.90	0	100.00	0.32
	473	57.5	81.00	21.50	13.00	8.50	60.00	0.30
	523	54.0	61.35	24.25	11.00	13.25	45.30	0.19
	573	53.4	55.88	26.00	5.00	21.00	19.23	0.16
Al-2.5wt%Al_2O_3	298	60.0	110.72	17.40	17.40	0	100.00	0.34
	473	59.30	72.60	18.70	10.00	8.70	53.5	0.24
	523	51.30	60.00	18.75	8.80	9.95	46.9	0.22
	573	45.96	50.80	16.00	5.20	10.80	32.5	0.20
Al-5wt%Al_2O_3	298	74.0	146.78	16.90	15.50	1.40	91.72	0.35
	473	73.67	89.61	20.80	14.30	6.50	68.75	0.25
	523	57.44	63.50	18.30	8.38	10.00	45.79	0.19
	573	36.84	40.30	20.60	7.50	13.10	36.4	0.14
Al-10wt%Al_2O_3	298	80.36	158.51	16.40	15.50	0.90	94.51	0.37
	473	80.74	90.72	28.00	10.75	7.25	38.39	0.28
	523	56.72	64.66	18.00	10.00	8.00	55.55	0.22
	579	28.75	30.97	9.40	4.60	4.80	48.93	…

T, deformation temperature; S_y, yield stress; S_u, tensile strength; El., elongation; ε_u, uniform strain; Post ε_u, post uniform strain; *n*, work-hardening exponent (initital hardening up to maximum load).

forcement weight fraction. In MMCs, barriers to dislocation motion consist of submicron solute atoms or impurities in the matrix material, matrix grain boundaries, and the hard brittle reinforcement particles. The decrease in work-hardening exponent as a function of temperature can be attributed to dislocation annihilation or activation of dislocation motion by mechanisms other than glide, for example, climb (Ref 20). Work hardening is the result of the plastic deformation of the ductile matrix, that is, it is matrix controlled. This explains why the effect of reinforcement weight fraction is insignificant compared to the effect of deformation temperature. Table 1 shows the mechanical deformation parameters including work-hardening exponents for all cases. These values were obtained by fitting the true stress-true strain data to the power law $\sigma = k\varepsilon^n$, where σ, ε, k, and n are the true stress, true strain, strength coefficient, and work-hardening exponent, respectively. The usual definitions were used for calculating true stresses and the corresponding true strains.

Also, the rate of initial hardening was strongly affected by the deformation temperature as can be seen from Fig. 3(a) to (d) and as indicated by the slope of the initial parts of the stress-strain curves. However, it does not seem to be significantly af-

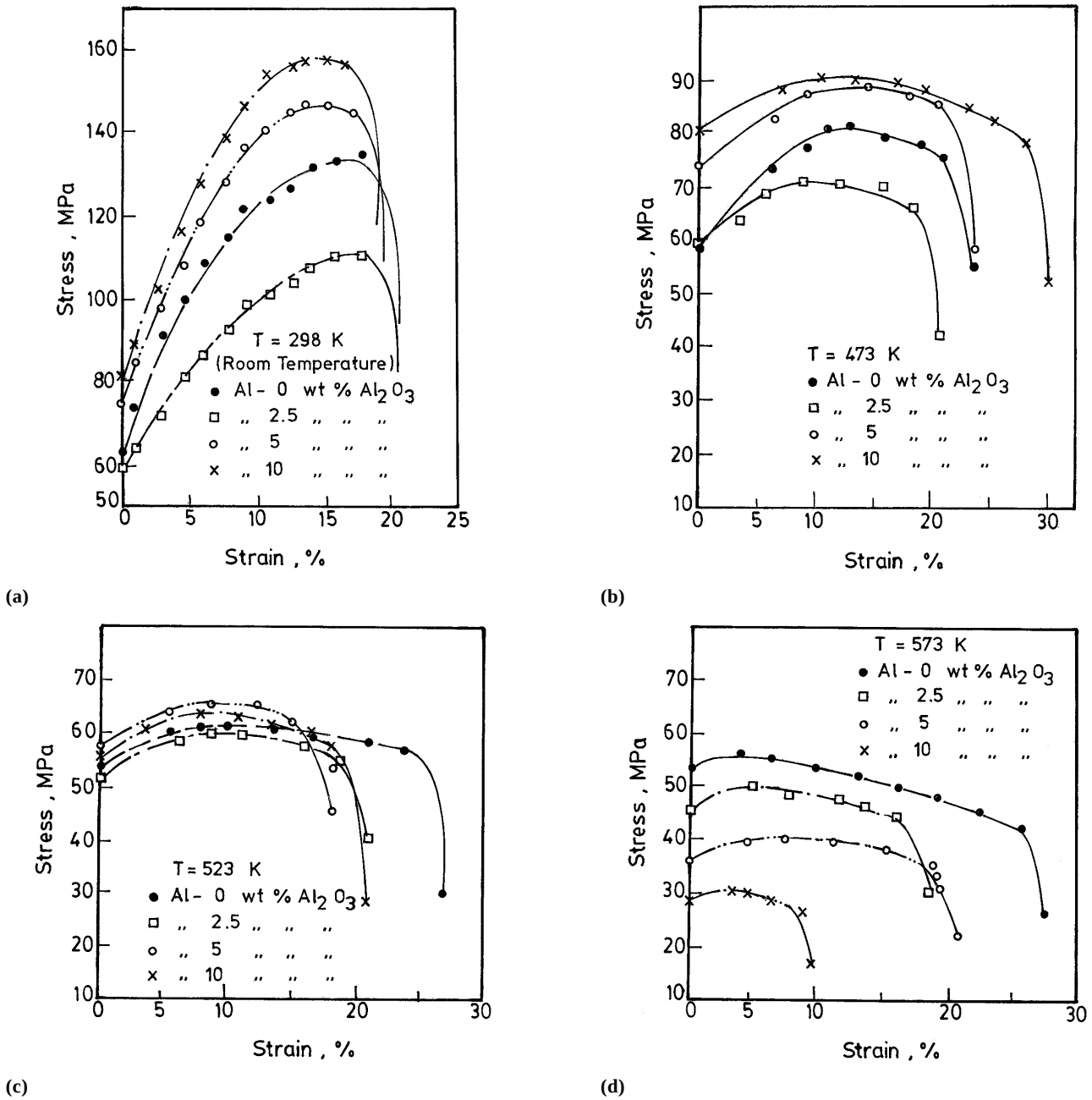

Fig. 2 (a) Conventional plastic stress-strain curves for Al-Al_2O_3 (room temperature). (b) Conventional plastic stress-strain curves for Al-Al_2O_3 (T = 473 K). (c) Conventional plastic stress-strain curves for Al-Al_2O_3 (T = 523 K). (d) Conventional plastic stress-strain curves for Al-Al_2O_3 (T = 573 K)

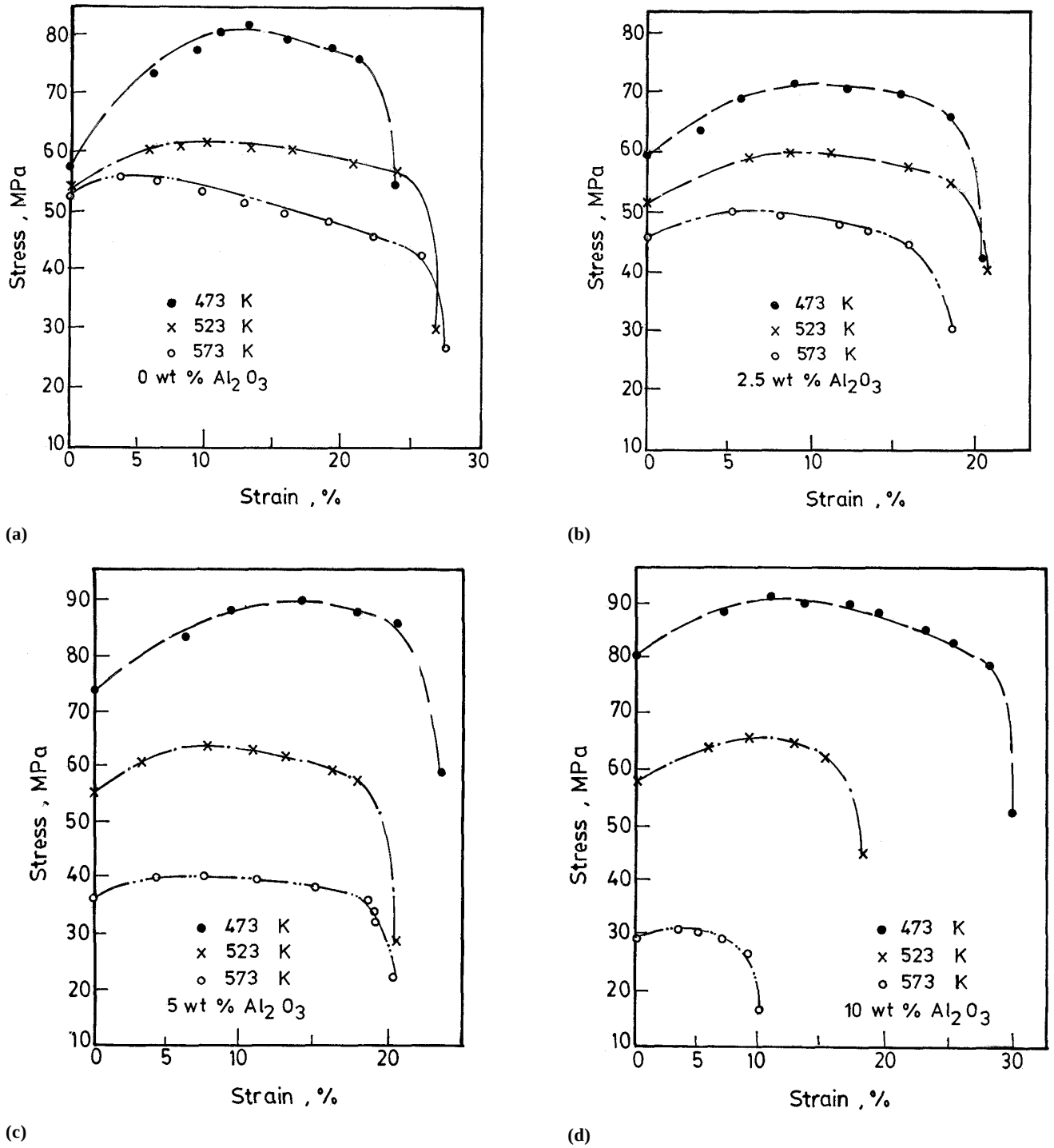

Fig. 3 (a) Conventional plastic stress-strain curves for Al-Al_2O_3 MMC (Al-0wt%Al_2O_3). (b) Conventional plastic stress-strain curves for Al-Al_2O_3 MMC (Al-2.5wt%Al_2O_3). (c) Conventional plastic stress-strain curves for Al-Al_2O_3 MMC (Al-5wt%Al_2O_3). (d) Conventional plastic stress-strain curves for Al-Al_2O_3 MMC (Al-10wt%Al_2O_3)

fected by the reinforcement weight fraction because all curves in Fig. 2(a) to (d) look parallel at the initial part of the curve. Thus, it can be concluded that both work hardening and rate of work hardening are matrix controlled.

Figures 4(a) and (b) show the variation of yield stress and tensile strength of the tested materials with deformation temperature. It can clearly be seen that two zones can be distinguished on the yield stress-temperature diagram. In zone I (temperature range 298 to 473 K), the yield stress is not affected by deformation temperature but is dependent only on material composition. This temperature range is equivalent to 0.32 to 0.5 T_m.

In zone II (temperature range 473 to 573 K, equivalent to 0.5 to 0.6 T_m), the yield stress is highly temperature dependent.

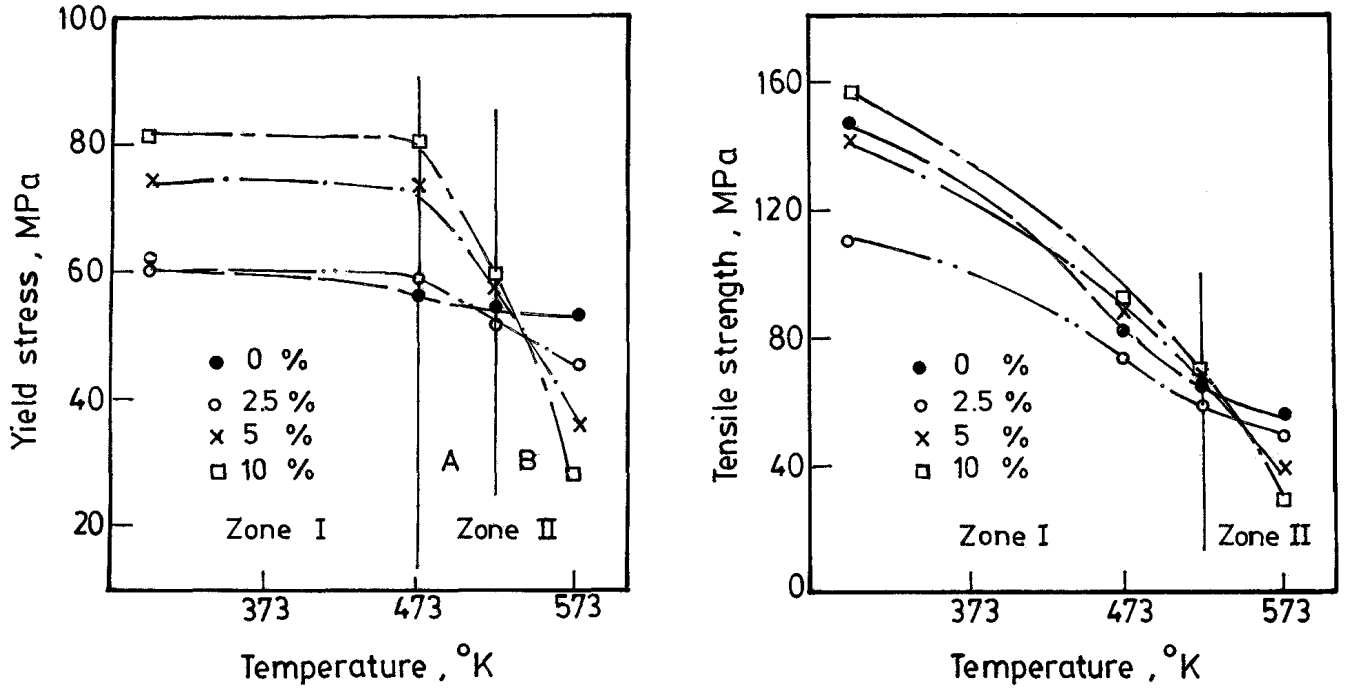

(a) **(b)**

Fig. 4 Variation of yield stress with deformation temperature. (b) Variation of tensile strength with deformation temperature

Sharp reduction in yield stress accompanied the increase in deformation temperature. Within zone II, two subzones, IIA and IIB, can be distinguished. In zone IIA the magnitudes of yield stress are ordered as $\sigma y_{10\%} > \sigma y_{5\%} > \sigma y_{2.5\%} > \sigma y_{0\%}$. In zone IIB the order is reversed, such that Al-10wt%Al_2O_3 has the lowest yield stress.

Figure 4(b) indicates that the tensile strength of the Al-Al_2O_3 MMC in the present work is both temperature and composition dependent for the entire temperature range considered. However, the deformation temperature dependency of the tensile strength is greater than that of the yield stress. Two zones can be distinguished on this diagram as well, zone I and II. The difference between the two zones is the order of arrangement of tensile strength magnitudes, which follows the same observation mentioned previously for yield strengths, zone IIB.

The effect of deformation temperature on the strength becomes more significant as more alumina weight fraction is added to the matrix. If the reduction in tensile strength for the different material compositions is compared between $T = 473$ K and 573 K, it is found that for the Al-0wt%Al_2O_3, Al-2.5wt%Al_2O_3, and Al-10wt%Al_2O_3, the reductions in strength are 32, 30, 55, and 65.8%, respectively, as compared to room temperature strength. This can be attributed to early nucleation of dynamic recrystallization in MMCs containing higher alumina weight fractions, which will be discussed in the following paragraphs.

Figure 5(a) shows the variation of elongation percent to fracture versus deformation temperature as a function of material composition. The elongation percent to fracture continued to increase monotonically for the unreinforced matrix as a function of deformation temperature. The rate of increase in elongation percent was slower for the Al-2.5wt%Al_2O_3 and Al-5wt%Al_2O_3 MMCs. The elongation percent for Al-10wt%Al_2O_3 increased between 298 and 473 K; afterward, it started to decrease at a steep rate to decrease by 35.7% at 523 K and by 67.8% at 573 K. The effect of reinforcement weight fraction on the ductility of MMCs results from the role of particle/matrix interface. The matrix material contained between reinforcement particles usually experience highly localized and concentrated stress distribution (Ref 21, 22). Such stress concentration could lead to cavitation at these interfaces (Ref 23), thus, terminating the ductility of the material. As reinforcement weight fraction increases, this effect becomes more significant.

Usually, elongation percent to fracture can be split into two main components: uniform elongation (starts at yielding and up to onset of necking or up to maximum load) and post-uniform elongation (from necking to fracture). Figure 5(b) shows the variation of uniform elongation with deformation temperature. It is clear that the uniform elongation ε_u decreased as a function of temperature and as the reinforcement weight fraction increased. Thus, the contribution of post-uniform elongation to total elongation increases as temperature increases and as reinforcement weight fraction increases, as shown in Fig. 5(c).

The effect of deformation temperature on elongation percent to fracture becomes apparent if the post uniform elongation for two cases of Al-10wt%Al_2O_3 is compared. At 573 K it comprised 51% of the total elongation to fracture, while at 298 K (room temperature) it comprised only 5% of the total elongation.

4.2 Hot Deformation Mechanisms

Softening during hot deformation is usually attributed to two main mechanisms: dynamic recovery and recrystallization (Ref 24). In dynamic recovery, entangled dislocations move and reorganize themselves into a more stable structure of

subgrains characterized by low angle grain boundaries (Ref 25). This process is usually accompanied by loss of strength with little or no improvement in ductility. Dynamic recovery occurs in metals of high stacking fault energy (SFE), for example aluminum and most body-centered cubic (BCC) metals (Ref 24). Dynamic recrystallization proceeds by dislocation annihilation, grain boundary migration, and grain growth. It is accompanied by a sharp drop in strength and significant improvement in ductility. Dynamic recrystallization is commonly observed in low SFE metals, for example, face-centered cubic (FCC) metals except aluminum (Ref 26).

Authors disagree on which softening mechanism occurs during hot deformation of aluminum, aluminum alloys, and aluminum-matrix MMCs. Olla and Virdis (Ref 24) found that in high temperature deformation of a commercially pure aluminum, the dominating softening mechanism is dynamic

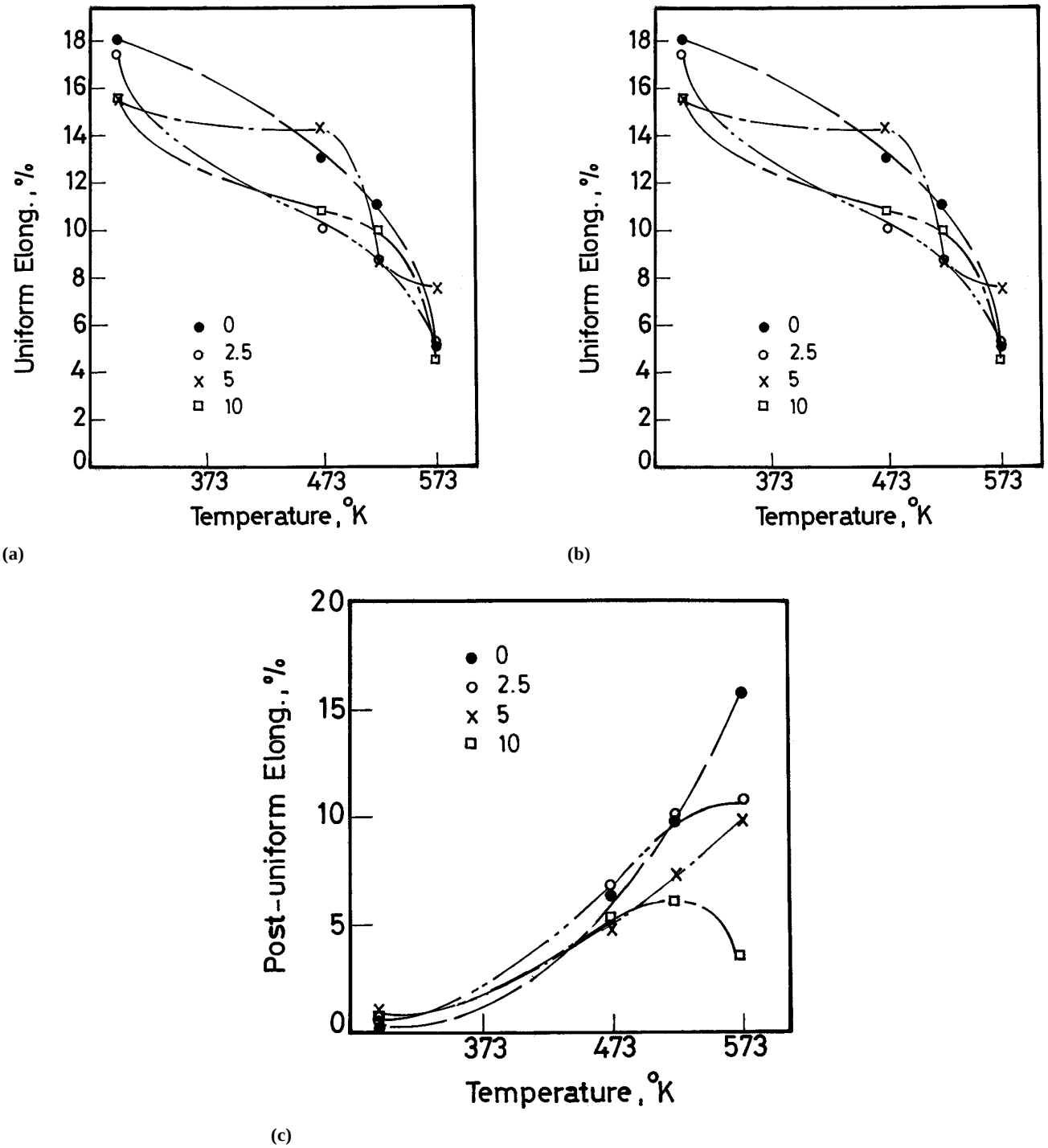

Fig. 5 (a) Variation of elongation percent with deformation temperature. (b) Variation of uniform elongation with deformation temperature. (c) Variation of post-uniform elongation with deformation temperature

recovery. This conclusion was based on the observation of subgrains in the microstructures of specimens elongated to fracture. The same conclusion was drawn by Sheppard and Zaidi (Ref 27, 28). McQueen et al. (Ref 29) reported dynamic recrystallization at 400 °C and 220 s^{-1} and complete recrystallization at 490 °C and 11 s^{-1}, in a commercially pure aluminum.

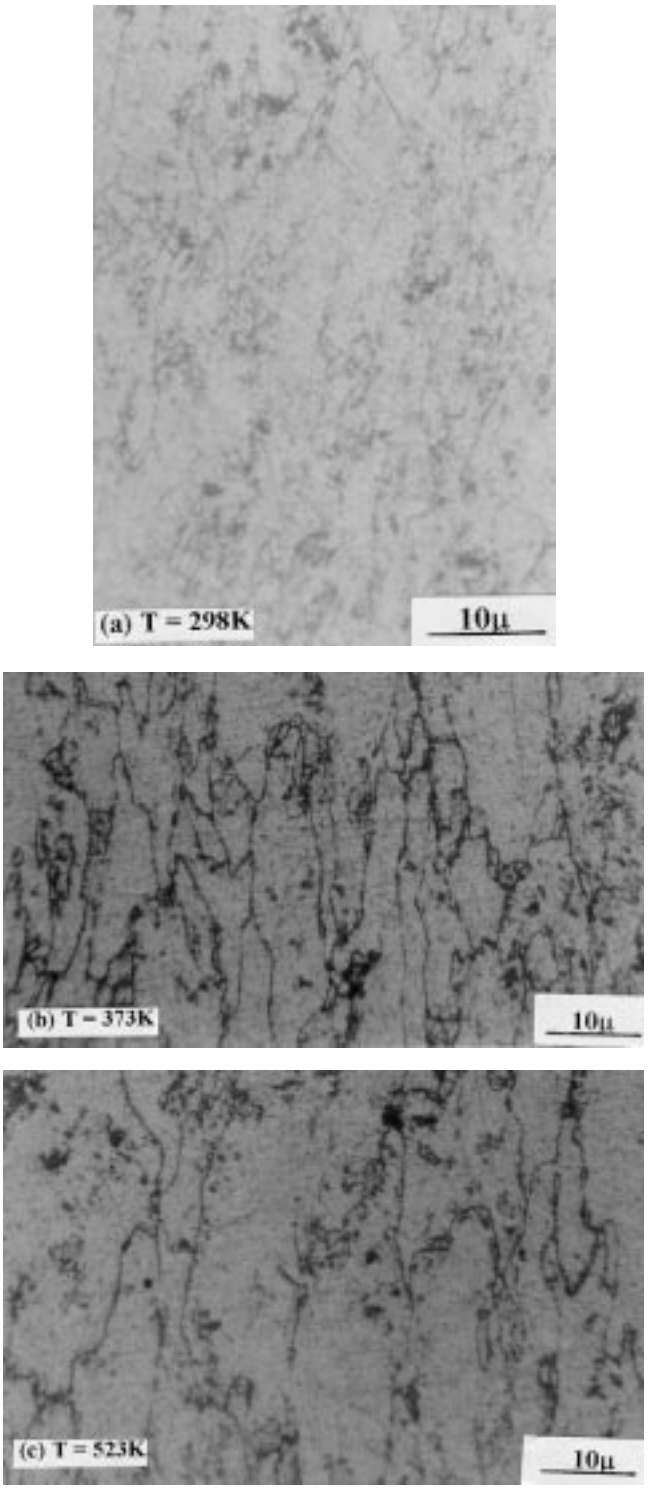

Fig. 6 Micrographs of Al-0wt%Al_2O_3 MMC. (a) T =373 K, small grain size dominates the microstructure, same observation at room temperature. (b) T = 473 K, grain substructures and partial recrystallization. (c) T = 523 K, complete dynamic recrsystallization. 1520×

In the present study, the micrographs of the unreinforced matrix showed small grain sizes at room temperature and up to 373 K. Small grains and low angle grain boundaries dominate the micrograph. Such features play a major role in accumulation of dislocations and dislocation entanglements. Thus, the stored strain energy at these grain boundaries is raised. At a deformation temperature of 473 K, the micrograph in Fig. 6(b) is dominated by grain substructures, although partially recrystallized grains can also be observed. These grain substructures are evidence of dynamic recovery. As the deformation temperature increased to 523 K, dynamic recrystallization dominates the micrograph. At 573 K, the microstructure experienced complete recrystallization (Fig. 6c). These observations are in excellent correlation with the mechanical testing results. The unreinforced matrix experienced a sharp drop in yield stress coupled with significant improvement in ductility at 573 K, while in the range 298 to 473 K the material continued to lose its strength at a slight rate and continued to gain more ductility. In the range of $473 < T_d < 573$, where T_d is the deformation temperature, dynamic recrystallization proceeded at a faster rate where it was completed at T_d = 573 K.

The role of second phase particles in aluminum and its alloys and their effects on the softening mechanisms during hot deformation has been examined by several authors (Ref 30-32). Sheppard et al. (Ref 30) and Sheppard and Tutcher (Ref 31) reported partial recrystallization in an Al-5wt%Mg alloy when extruded at 450 °C at a ratio of 40 to 1. As the solute content increased, the fraction of microstructure that experienced dynamic recrystallization increased. Zhong et al. (Ref 33) observed that recrystallized grains were found in the microstructure of a 5083 aluminum alloy near large insoluble chromium, iron, and manganese rich particles. The role of high concentration of solute atoms in inducing dynamic recrystallization was explained in two ways: solute atoms are believed to hinder the dislocation motion, thus, increasing the stored strain energy, which promotes recrystallization nucleation (Ref 33). The other explanation is that solute atoms reduce the SFE of the material (Ref 34), thus increasing the driving force for dynamic recrystallization. However, Sheppard et al. (Ref 30), Sheppard and Tutcher (Ref 31), and McQueen et al. (Ref 29) argued that the role of solute atoms in reducing SFE is not obvious.

From this discussion, the role of second phase particles in promoting dynamic recrystallization during hot deformation can be explained in two ways: (a) second phase particles strongly bonded to the matrix are effective barriers to dislocation motion leading to accumulation and entanglements of these dislocations and (b) the presence of second phase particles leads to finer grain sizes with larger grain boundary surface area. Both ways lead to raising the stored strain energy, thus, promoting dynamic recrystallization rather than dynamic recovery during hot deformation.

In the present study, the Al-2.5wt%Al_2O_3 MMC exhibited dynamic recovery when deformed in the temperature range 373 to 473 K. This can be verified by the presence of subgrain structures. However, above 523 K, dynamic recrystallization was dominated by grain growth and grain boundary migration (Fig. 7c). The absence of grain substructures from the micrographs

verifies this conclusion. Similar observations were noted for the Al-5wt%Al_2O_3. As the reinforcement weight fraction increased to 10 wt% Al_2O_3, the grain structure became finer, and dynamic recrystallization was observed at a deformation temperature, T = 473 K (Fig. 8b), that is, the material showed early nucleation of recrystallization. Thus, it can be concluded that the softening mechanisms in Al-Al_2O_3 MMC manufactured by PM techniques are structure and temperature dependent. The main structure parameter controlling the softening mechanism is the grain size, which is controlled by the processing route and

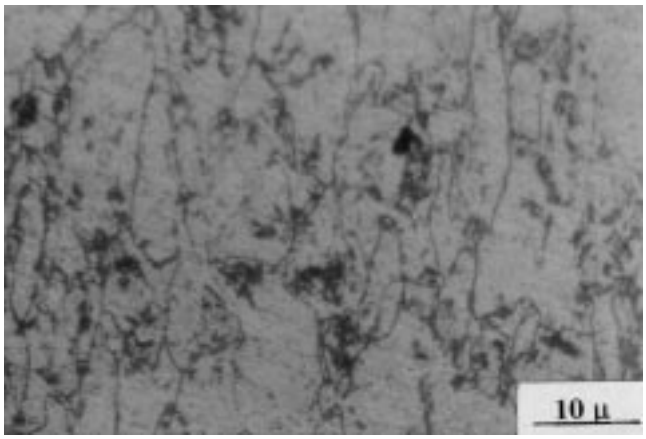

(a)

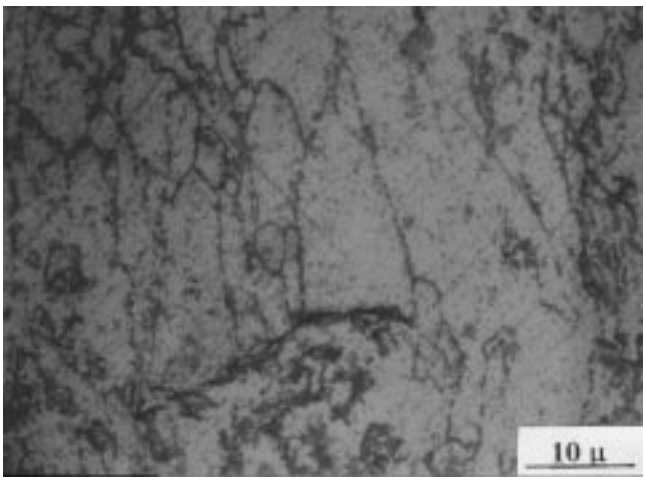

(b)

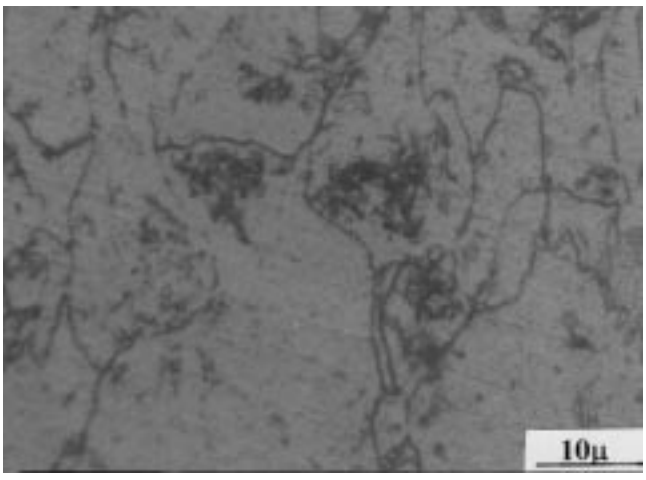

(c)

Fig. 7 Micrographs of Al-2.5wt%Al_2O_3 MMC. (a) T =373 K, dynamic recovery (grain substructure). (b) T = 473 K, dynamic recovery with partial dynamic recrystallization. (c) T = 523 K, dynamic recrystallization. 1520×

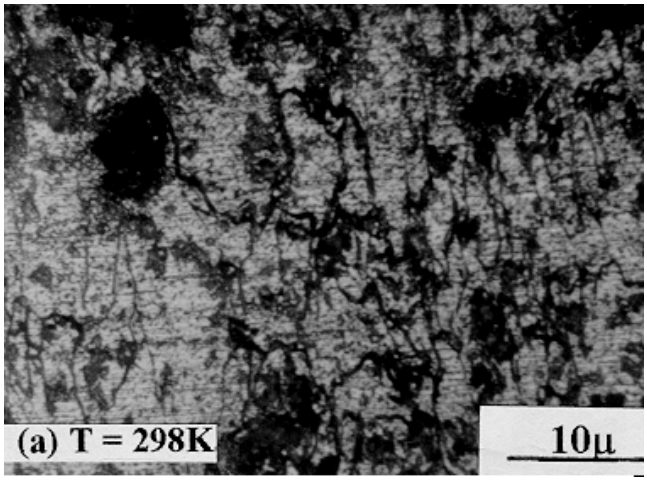

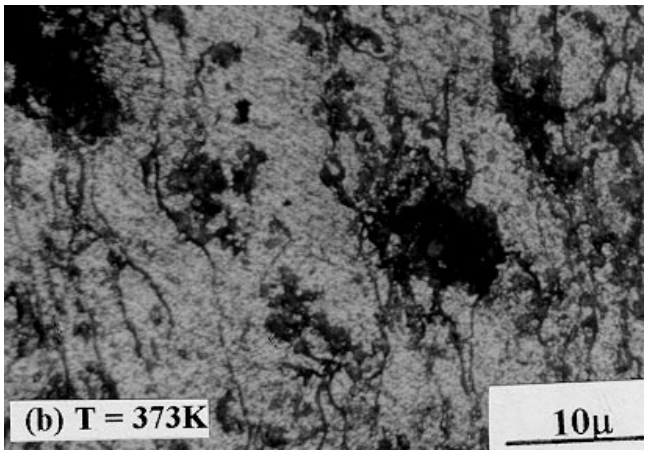

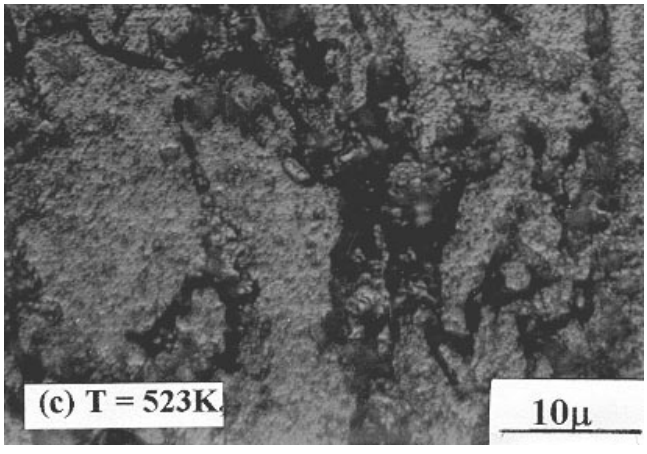

Fig. 8 Micrographs of Al-10wt%Al_2O_3 MMC. (a) T =373 K, room temperature microstructure. (b) T = 473 K, dynamic recovery with and dynamic recrystallization. (c) T = 523 K, complete dynamic recrystallization. 1520×

reinforcement weight fraction. For lower reinforcement weight fractions, the matrix is decisive.

In the analyzed microstructures, the Al_2O_3 particles were found to be located inside the recrystallized grains or near the grain boundaries. This indicated that Al_2O_3 particles presented favorable sites for nucleation of recrystallization; however, nucleation could also occur at grain and subgrain boundary junctions. Humphreys (Ref 35) and Miller and Humphreys (Ref 36) suggested that each reinforcement particle nucleated one grain. Zhong et al. (Ref 33) found that each reinforcing particle nucleated several grains. So the role of reinforcement particles in recrystallization nucleation is significant. In the present work, it was not possible to establish a clear relationship between the number of grains nucleated due to each reinforcing particle.

5. Conclusions

The following conclusions can be drawn:

- The high temperature deformation behavior of Al-Al_2O_3 MMCs of different reinforcement weight fractions starts by initial hardening at low strains—up to a maximum load followed by softening.
- The rate of initial hardening is strongly affected by the deformation temperature. However, it does not seem to be strongly affected by the reinforcement weight fraction.
- In the temperature range of 298 to 473 K, the yield stress of an MMC is composition and temperature independent. In the temperature range 473 to 573 K, the yield stress is highly temperature dependent.
- The tensile strength of the MMC is highly temperature and composition dependent over the entire range of deformation temperatures investigated. The effect of deformation temperature is more significant for higher reinforcement weight fractions.
- Both dynamic recovery and dynamic recrystallization were observed to operate for the high temperatures used. For the unreinforced matrix, dynamic recovery dominated up to 473 K, but as the temperature reached 523 K, dynamic recrystallization became more dominant. This same trend was observed for the MMC containing up to 5 wt% Al_2O_3. For Al-0wt%Al_2O_3 dynamic recrystallization started at 473 K, that is, the increase in reinforcement weight fraction lead to early nucleation of recrystallization.
- The observed microstructural features are in good agreement with the mechanical testing results.

References:

1. G.E. Dieter, *Mechanical Metallurgy,* 2nd ed., McGraw Hill, 1988, p 432
2. K.N. Ramakrishnan, H.B. McShane, T. Sheppard, and E.K. Jonnidis, *Mater. Sci. Technol.*, Vol 8, 1992, p 709
3. Y.W. Kim, in *Dispersion Strengthened Aluminum Alloys,* Y.W. Kim and W.M. Griffith, Ed., TMS, Warrendale, PA, 1988
4. T.E. Teitz and I.G. Palmer, *Advances in Powder Technology,* American Society for Metals, 1982
5. R.A. Signorelli, Progress in Science and Engineering of Composites, T. Hayashi, K. Kawata, and S. Umekawa, Ed., ICCM-IV, Tokyo, 1982, p 37
6. R.B. Bahgat, Metal Matrix Composites: Processing and Interfaces, R.K. Everett and R.J. Arsenault, Ed., Academic Press, 1991, p 43
7. A.K. Dhingra and L.B. Gulbransen, *Cast Reinforced Metal Matrix Composites,* S.G. Fishman and A.K. Dhingra, Ed., ASM International, 1988, p 271
8. S.J. Harris, *Mater. Sci. Technol.*, Vol 4, 1988, p 231
9. S. Ray, *J. Mater. Sci.*, Vol 28, 1993, p 5397
10. R.M. Bhagat, M.F. Amateau, M.B. House, K.C. Meinert, and P. Nisson, *J. Compos. Mater.*, Vol 26 (No. 110), 1998, p 1578
11. M. Manoharan and J.J. Lewandowski, *Mater. Sci. Eng. A,* Vol 150, 1992, p 179
12. J. Singh, S.K. Goel, V.N.S. Mathur, and L.M. Kapoor, *J. Mater. Sci.*, Vol 26, 1991, p 2750
13. S.W. Lai and D.D.L. Chung, *J. Mater. Sci.*, Vol 29, 1994, p 6181
14. N.J. Abdul-Latif, A.I. Khedr, and S.K. Goel, *J. Mater. Sci.*, Vol 22, 1987, p 466
15. A.H. Cottrell, *An Introduction to Metallurgy,* Edward Arnold, London, 1967, p 402
16. C.M. Friend, *J. Mater. Sci.*, Vol 22, 1987, p 3005
17. K.S. Aradhya and M.K. Surappa, *Scr. Metall. Mater.*, Vol 25, 1991, p 817
18. A.A. Mazen and A.Y. Ahmed, *Proceedings of the Fifth Int. Conf. on Composites Engineering, ICCE/5* (Las Vegas, NV), July 1998, p 607
19. M.J. Haynes and R.P. Gongloff, *Metall. Mater. Trans. A,* Vol 28, 1997, p 1815
20. D.G.C. Syn and A.K. Ghosh, *Metall. Mater. Trans. A,* Vol 25, 1994, p 2049
21. R.J. Arsenault, N. Shi, C.R. Feng, and L. Wang, *Mater. Sci. Eng. A,* Vol 131, 1991, p 55
22. W.M. Zhong, G. L'Esperance, and M. Suery, *Mater. Sci. Eng. A,* Vol 214, 1996, p 104
23. A.F. Whitehouse and T.W. Clyne, *Acta. Metall. Mater.*, Vol 41 (No. 6), 1993, p 1701
24. P. Olla and P.F. Virdis, *Metall. Trans. A,* Vol 18, 1987, p 293
25. O.D. Sherby, R.H. Klundt, and A.K. Miller, *Metall. Trans. A,* Vol 8, 1977, p 843
26. H.T. McQueen, W.A. Wang , and J.J. Jonas, *Can. J. Phys.*, Vol 45, 1967, p 1225
27. T. Sheppard and M.A. Zaidi, *Met. Technol.*, Vol 9, 1982, p 52
28. M.A. Zaidi and T. Sheppard, *Met. Sci.*, Vol 16, 1982, p 229
29. H.J. McQueen, E. Evangelista, J. Bowels, and G. Crawford, *Met. Sci.*, Vol 18 (No. 8), 1984, p 392
30. T. Sheppard, N.C. Parson, and M.A. Zaidi, *Met. Sci.*, Vol 17 (No. 10), 1983, p 481
31. T. Sheppard and M.G. Tutcher, *Met. Sci.*, Vol 14 (No. 12), 1980, p 579
32. S.J. Hales and T.R. McNelley, *Acta Metall.*, Vol 36, 1988, p 1229
33. W.M. Zhong, E. Goiffon, G. L'Espérance, M. Snéey, and J.J. Blandin, *Mater. Sci. Eng. A,* Vol 214 ,1996, p 84
34. A.R. Jones, *Grain Boundary Structure and Kinetics,* American Society for Metals, 1980, p 373
35. F.J. Humphreys, *Proc. 9th Riso Symp.*, S.I. Anderson, H. Lilhst, and D.B. Pedrson, Ed., Denmark, 1988, p 51
36. W.S. Miller and F.J. Humphreys, *Scr. Metall. Mater.*, Vol 25, 1991, p 33